http://dx.doi.org/10.5012/bkcs.2012.33.10.3397

Growth Mechanism and Crystal Ordering of Spherulitic Patterns in a Belousov-Zhabotinsky Type Reaction System

Narendra Yadav,[*] S. S. Majhi,[†] and P. K. Srivastava[†]

Department of Space Engineering & Rocketry, Birla Institute of Technology, Mesra, Ranchi
[*]E-mail: yadav_chemistry@rediffmail.com
[†]Department of Applied Chemistry, Birla Institute of Technology, Deoghar Campus, Deoghar
Received June 13, 2012, Accepted July 25, 2012

Three types of spherulitic morphologies have been investigated in dual substrate mode of Belousov-Zhabotinsky (BZ) type reaction system. Prior to growth of spherulites, three distinct patterning behaviors have been observed sequentially during the reaction process. Initial and the early-phase of reaction showed the emergence of concentric ring-like wave patterns. A colloidal-state of reaction consists of numerous fine solid particles, which forms primarily some nucleation centers of dendritic characters. The nucleation centers were found to grow in sizes and shapes with the progress of reaction. It leads to growth of dendritic-like spherulitic crystal patterns. The resultant spherulites showed transitions in their morphologies, including sea-weeds and rhythmic spherulitic crystal patterns, by the effects substituted organic substrate and in the higher concentration of bromate-initiator respectively. The branching mechanism and crystal ordering of spherulitic textures were studied with help of optical microscope (OPM) and scanning electron microscope (SEM). Characteristics of crystal phases were also evaluated using X-ray diffraction (XRD) and differential thermal analysis (DTA). Results indicated that the compositions of reactants and crystal orderings were interrelated with morphological transitions of spherulites as illustrated and described.

Key Words : Reaction-diffusion, Spherulites, Self-assembly, Inter face, Crystal ordering

Introduction

Non-equilibrium crystallization phenomena can be considered as the process of molecular self-assembly, resulting in fascinating crystal patterns such as dendrites and spherulites.[1-3] The dendrites exhibit a hierarchical microstructure, which is often observed in growth processes of a number of metallurgic or alloys, inorganic and organic material systems. On the other hand, the spherulites are radially oriented micro-crystals, considered to be centrally nucleated which grow as spherical and radial symmetric crystal patterns. These crystal forms are important and ubiquitously observed in many functional materials during their processing conditions. In recent decades, the spherulitic crystal patterns are extensively studied in polymers,[4,5] liquid crystals,[5,6] proteins,[6,7] metallurgical alloys[2,3] and some biological relevance's.[8-10]

The mechanism of the formation of spherulitic patterns may not be related to specific details of molecular characteristics. Depending on the chemical parameters (molecular geometry, molecular weight *etc*.) and physical properties (crystallization kinetics, crystalline lattice *etc*.), a number of spherulitic morphology has been recognized. The surface energy, nucleation kinetics, driving force, surface anisotropy *etc*., are the other factors which can influence the crystal orderliness and morphologies of the spherulites. Self-organization among crystal entities has been also found effective, to control the orientations and hierarchy of growing patterns.[10-12] When growing components fall in the range of micro- or nano-scales, the structure of the patterns may be affected by some short range molecular interactions, hydrophobic, hydrophilic, gravitational, van der-Waals, and Coulombic forces *etc*. However, all these patterns share a common category of pattern formation and their morphologies include spherulites, dendrites, diffusion limited aggregation (DLA)-like patterns and densely branched morphology (DBM).[1,2,13]

Apart from this, it has been demonstrated that some chemical systems occasionally show periodic changes of their concentrations in space or time at far from equilibrium conditions which gives rise to various spatiotemporal patterns. The BZ reactions and Leisegang's patterns are two well characterized examples of such pattern forming systems.[14-17] Pattering features of these two typical phenomena which comprises, concentric rings, target waves, spiral bands *etc.*, have largely been characterized by the occurrence of chemical oscillation and interrelation of reaction-diffusion mechanism between its molecular constituents. The existence of oscillations in non-equilibrium crystallization processes which leads to growth of some spontaneous and periodic branching crystal patterns have also been exemplified. The importance of chemical oscillation has recently been shown in the growth of symmetric-dendritic patterns. These crystallizing systems reasonably resemble with excitable media and their growth front seems to propagate as wave, which is generally observed in an oscillatory chemical reaction. From this point of view, the basic reaction-diffusion mechanism must be considered in the formation of coherent and symmetric

crystal patterns, quite similar to cycles of oscillation. Thus, striking similarities can be anticipated between oscillatory systems and the patterns of non-equilibrium crystallization process.

In the present investigation, the growth behaviors of spherulitic crystal patterns during BZ reaction process have been studied. An effort has been made to explicate the role of reaction-diffusion in crystal ordering of spherulites. Self-assembly mechanism has also been proposed to show the crystal organization of spherulitic textures. Different morphological transitions of spherulites were undertaken in this study. It shows that the growth of spherulites and crystal ordering were concentration dependent. Morphological transitions of spherulitic forms were correlated with concentration profile of some key reactants. Possible spherulitic crystal phases were characterized by optical microscope, scanning electron microscope, X-ray and thermal analysis and their results have been used to explain the phase transitions of spherulites.

Experimental

Materials and Stock Solutions. Succinic Acid (SA), acetyl acetone (AA), Succinic anhydride (SAA) and iron (II) sulphate (CDH India Ltd.), sulphuric acid (98%) of S.D. fine chemicals, India Ltd., 1,10-phenanthroline, ammonium cerium (IV) sulphate, and potassium bromate ($KBrO_3$) (E-Merck) of analytical grade were used for experimentation. All the experiments were performed in a flat Petridis of 9.1 cm (id). The experimental table and set-up was leveled and checked by sprit-level. Stock solutions of SA (5% w/v), SAA (5% w/v), [AA] = 1.59 mol dm^{-3} and ferroin [[Fe $(Phen)_3]^{2+}$] = 0.025 mol dm^{-3} was prepared in doubly distilled water (DDW). The ferroin is a redox indicator which was prepared by homogenous mixing of 1,10-phenanthroline and iron (II) sulphate in a molar ratio of 3:1 in DDW. Stock solution of the $KBrO_3$ and ammonium cerium (IV) sulphate (Ce^{4+}) (5% w/v) were prepared in H_2SO_4 = 1.5 mol dm^{-3}.

Instrumental Analysis. The studies of morphology and structure of the crystal patterns were carried out by optical microscope (OPM) (Leica, EZ4D) at a specific magnification and scanning electron microscope (SEM) (Jeol, JSM 6390LV) coupled with energy dispersive spectrum (EDS), at low vacuum of accelerating voltage of 20 kV. Thermal analysis of the spherulitic crystal materials were carried out by TGA/DTA techniques (Shimadzu DTG-60, Japan) in the range of 0 to 500 °C. The particle size analysis was carried out by Dynamic Light Scattering (DLS) technique (Malvern, Zeta-Sizer NANO ZS). The crystal materials were characterized by X-ray powdered diffractometer (Rigaku, Model, Miniflex-2005B111) equipped with Cu Kα (λ = 1.54 Å) operating at a tube load 100 V: 10 A and 50/60 Hz. Each sample was scanned in (2θ) range between 10° to 80° with a scan rate of 0.2°/3 sec.

Synthetic Procedures. A solution was prepared by mixing 2 mL of SA, AA, Ce^{4+} and H_2SO_4, along with 1.0 mL of ferroin ($[Fe(Phen)_3]^{2+}$) in a 250 mL beaker and was made homogenous by constant shaking. Then 2 mL of the $KBrO_3$ solution was added to resultant mixture. It was well shaken to maintain the homogeneity of the reaction solution. The introduction of $KBrO_3$ into the rest of solution mixtures was marked as initiation of reaction process. Thereafter, 6.5 mL of solution mixtures was immediately taken out from bulk solution and spread in a Petridis, which makes a thin layer of reaction solution of uniform thickness (~1 mm) with Petridis. The resultant concentrations of reactants were calculated as [AA] = 0.284 mol dm^{-3}, [SA] = 0.121 mol dm^{-3}, [Ce^{4+}] = 0.0122 mol dm^{-3}, [$KBrO_3$] = 0.0612 mol dm^{-3}, [$[Fe(Phen)_3]^{2+}$] = 0.00208 mol dm^{-3}, and [H_2SO_4] = 0.85 mol dm^{-3}.

When requisite quantities of reaction solution are poured into Petridis, a homogenous red color solution was appeared. After, a short steady state (~5 min), centrally a single blue nucleation occurred. It emanated from a point source producing a circular wave front which propagated outwardly with uniform speed. The repeating process led to the formation of concentric circles that further organized into a concentric rings-like pattern. This phenomenon continued for approximately 25 min. and, these ring patterns gradually starts to disappear from the outer sides and the reaction mixture returned to its reduced state (red color). This state remained static for nearly 10 min. Subsequently, a single blue nucleation was yet again observed on the red color reaction solution at the center. It was found to propagate in almost radial direction of the said solution media. Approximately 40 min. was taken to cover the whole surface area of the Petridis (4.55 cm (id)). After completion of this process the reaction solution completely transformed into blue color which remained static for the next 7 hours. A colloidal phase which composed of numerous fine solid particles embedded in the solution matrix was observed after 7 hours. These colloidal particles self-assembled to form some discrete crystal points, called nucleation centers. The nucleation centers exhibits ordered crystal patterns of dendritic character. With the progress of reaction, the nucleation centers were found to increase in size by the self-assembly among the product crystal components and finally the spherulitic crystal patterns have resulted.

Results and Discussion

The growth of spherulitic crystal patterns were observed after some successive reaction processes. These reactions show complex patterning behavior of distinct quality However, they possess a common characteristic for subsequent reaction process. In order to simplify the complexity of the patterns formation, the present study has been studied with following distinguishable sections, namely solution-phase reaction, growth of spherulites, and growth forms of spherulites under the influence of substituted organic substrate and effect of initiator (BrO_3^-). Additionally, all possible crystal patterns were characterized with the help of OPM, SEM, DTA, DLS and XRD techniques. Based on these, the specific details of physico-chemical aspects of spherulitic structures

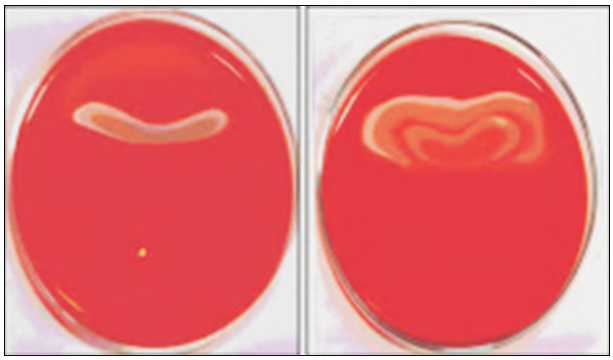

Figure 1. Concentric rings-like wave patterns.

have been presented.

Solution-Phase Reaction. The phenomenon which leads to emergence of concentric rings-like pattern and propagation of single wave front has been observed during solution-phase reaction as shown in Figure 1. These have striking similarity to target and spiral wave patterns of oscillatory reaction systems. They can reasonably be related to dual frequencies oscillations of typical BZ reaction. The high frequency are attributed to development of concentric ring-like patterns, while single blue wave front propagation may be said to form in the range of the low frequency regime of the present reaction. The redox reaction and reaction-diffusion phenomena were anticipated to control the periodic behaviors of the these reaction processes.

In the explanation of these two sequential pattern formation, the role of ferroin must be considered. In general, the ferroin acts as a redox indicator which can intensify the colour variations under the effect of the reaction-diffusion mechanism of the BZ reaction systems. The colour variations between red to blue indicates the states of the reaction solution *i.e.* reduced state (red colour) and oxidized state (blue colour) respectively. The coloration mechanism is helpful to analyze the emergence of waves and spatio-temporal patterns visually. The chemical structure of ferroin can changes their forms possibly between two states, as shown below,

$$\underset{\text{(Ferroin)}}{[Fe(phen)_3]^{2+}} \underset{\text{Reduced state}}{} \rightleftharpoons \underset{\text{(Ferriin)}}{[Fe(phen)_3]^{3+}} \underset{\text{Oxidized state}}{}$$

Moreover, the detailed mechanism and description for patterns formation can be explained by fundamentals of BZ chemistry.[18-23] This suggested that under traces of Ce^{4+} (or Fe^{2+}) and the presence of acidic BrO_3^- medium, the AA (or SA) can be oxidized. Some intermediates have also been formed whose concentrations were varied with function of time in periodic mannered. The RD mechanism may relocate new product phases and disperse them at regular intervals. However, the present reaction has becomes much complicated, because it is accompanied by a number of reaction events, *viz.* solution-phase reaction, solid-state nucleation, crystal growth and is followed by colloidal-phase. Instead, the qualitative aspects of patterns formation and chemistry of the present studies have been summarized in our earlier report.[24,25] Based on this, three stable products have been proposed through Scheme-I, in the Figure 2, which served as precursor for spherulitic crystal growths.

The product (A) and the product (B) are the bromo-derivatives and (C) is the hydroxyl derivative of the acetyl acetone (AA). These products may result from a series of reaction steps. Since, AA does not react directly with acidic BrO_3^-, but it can favorably reduced into HOBr by the reactions with Br^-/Ce^{3+}. This is an intermediate HOBr and can readily form products A, B and C by the reaction with AA. The stoichiometry of the reaction were effectively maintained by formation of some side reaction intermediates (Br^-, $HBrO_2$, $BrO_2^{\bullet}$, Br_2, *etc.*) as discussed.[25,26] Based on the reaction behaviors, the oscillatory cycles of the present reaction has been are summarized as; the AA is initially oxidized, the concentration of product A and B increases significantly. It confirmed by red-colored (reduced state) solution. These reaction steps can slow down the auto-catalytic oxidation of Ce^{3+} and oxidation reaction of AA. Thus, the reaction may proceed towards formation of product C. The concentration of product C is supposed to increase as the reaction progresses. The BrO_3^- is a key reagent for all types of BZ type reaction which initiates the reaction at the beginning and provides an oscillatory network by forming a number of intermediates. The concentration of these intermediates significantly controls the oscillatory behavior of solution-phase BZ reaction. Among them, the Br^- and $HBrO_2$ were two effective intermediates which played significant role in completing the cycles of oscillations. In the high concentration of Br^- ions, the reaction remained in reduced state where AA/SA starts to consume them simultaneously, and Ce^{3+} ions got oxidized. A by-product

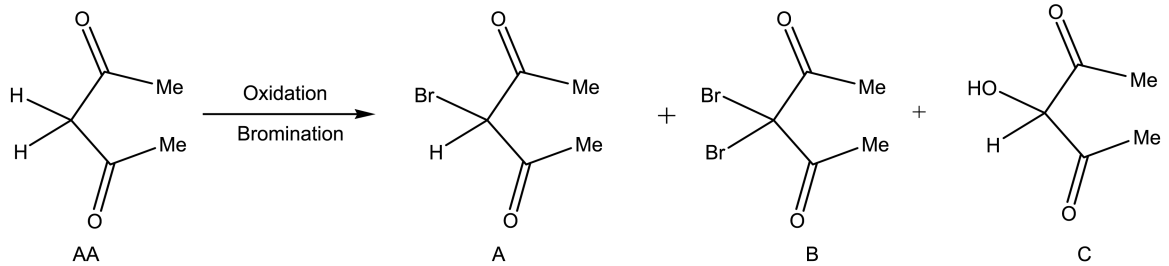

Scheme-I

Figure 2. Possible products of solution-phase reaction.

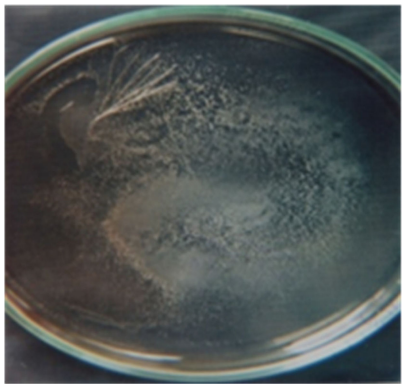

Figure 3. Colloidal-phase and solid state nucleation.

($HBrO_2$) was also formed during course of reactions. When $HBrO_2$ starts to diffuse into neighboring regions, concentration gradients between reduced and oxidized states fluctuated. This resulted into development of wave fronts which consists of oxidizing phase and reducing phase of the reaction. In general the reducing phase diffuses and propagates just after the oxidizing phase waves. Sometimes, the concentration of $HBrO_2$ had reached its higher level, which could inhibit the oscillation cycles. This facilitates to formation of Br_2 which could also transform the reaction into oxidized state.[20-23] Thus a cyclic reaction network was established between reduced state and oxidized state.

Growth of Spherulitic Crystal Patterns. After 7 hours, the reaction system showed colloidal-state, which composed of numerous fine solid particles embedded in the matrix of the reaction solution. These colloidal particles were self-aggregated into some discrete crystal centers termed as nucleation centers. Each nucleation center has been found to be surrounded by huge number of colloidal particles as depicted in Figure 3. These particles were diagnosed by SEM which reveals different shapes and geometries. Similarly, a number of products have been estimated during the nucleation process, as suggested in Scheme-I of the Figure 2. Under this, two intrinsic properties of the present reaction *viz.* excitability and instabilities have been considered which can be inducing the nucleation process. A concentration gradient was supposed between nucleation centers and uniformly distributed fine solid particles. This lead to formation of an orderly and symmetric nucleation structure followed by diffusive growth mechanism.[1-3] The excitability (tends to return back in its nearest steady state) is a key character of BZ-like reactions. In the non-equilibrium condition, excitability further supported to the Mullins-Sekerka type of dynamic instability. These two factors acting together may provide a fluctuating media where nucleation center grew orderly and symmetrically.

Based on the Scheme-I, the multi-product phases have been estimated. Obviously, these have different values of diffusion coefficients. It can control the mobility of diverse crystals to fuse together or attach with interfaces. The surface anisotropy might be seen in the growing nucleation structures. This is due to the presence of multi-product phases of different geometries and different values of their mobility. In this way, disorderliness in the growing structure may be obtained. Addition of some rudimentary crystals in the structure might form some meso-scopic crystal surfaces. It has been examined that the meso-scopic crystals when added to the growing structure, their surface energy increases and order of crystallographic symmetry is lowered. The metal catalysts (Ce/Fe ions) presented in the solution matrix may further destabilize their symmetry into new crystallographic angles. This is because the metal ions have both non-uniform crystal surfaces and well defined crystallographic symmetry.[27] Thus, an orderly nucleation structure have resulted.

As discussed, the meso-scoic crystals were facilitating to form dendritic nucleation structures. It is elaborated by using "particle-mediated crystallization theory", which emphasizes on how transformation of crystal phases takes place during nucleation phenomenon. The rudimentary crystals were initially self-assembled to form some orderly meso-crystals. When two or more number of meso-crystals fused together, a single crystal was formed with specific shape and size. During this process, the self-assembly process must be undertaken among the meso-scopic crystals which restrict them in the way that, their crystallographic symmetry is maintained in all the directions.[28] When the stable nucleation structure was formed, it started to grow in size and shape and, in stipulated directions that acquired the form of spherulitic crystal patterns. It is observed that the spherulitic crystal start to grow radially from their nucleation site. The fibrillar crystals were found to be branching intermittently which retained space-filling characters uniformly. A schematic growth mechanism of nucleation structures has been illustrated in Scheme-II of the Figure 4. The typical morphology of fully grown spherulitic crystal patterns has been presented in the Figure 5. They closely resemble the polymeric spherulites of the category-I. Overall growth mechanism of spherulitic crystal patterns has been illustrated through graphical Scheme-III, as shown in the Figure 6.

The spherulites have appeared in entirely spherical geometries. This geometry could result from a complex interplay between heat and mass transfer within the reaction media.[2,13] The phase field theory (PFT) of Granasy *et al.* suggested that spherical shapes of spherulites might be due to the growth front nucleation (GFN). They showed that the new crystal grain is nucleating at the surface of parent crystal

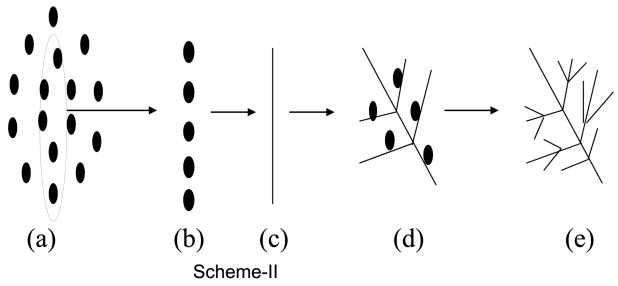

Figure 4. Schematic representation of self-assembly nucleation mechanism.

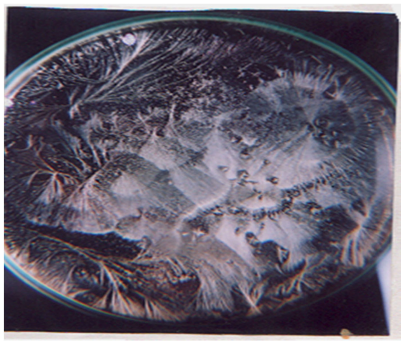

Figure 5. Typical morphology of spherulitic crystal patterns.

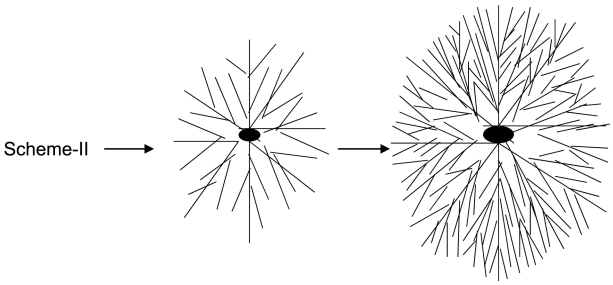

Figure 6. Schematic illustrations of spherulitic crystal growth.

at specific lattices. The randomization and orientation among new crystals were frequently undertaken to monitor the isotropy of spherical geometry at larger scales and longer duration. Because of metallic traces (ions), the long lived dynamic heterogeneity is helpful in restricting the crystals units to agglomerate. They were suited to provide sites for multiple growth front nucleation. The disorder in the growing structure emerges *via* GFN and multi-crystal phases.[1] Multiple GFN leads to the randomization of crystal units in directions of the crystallographic symmetry which is essentially maintained the isotropy of resultant structures. If the disorder is sufficiently large, the growing interfaces were started to orientate in the low crystallographic symmetry. It results in a robust spherical crystal patterns. Concurrently, the self-organization among the crystal units have undertaken towards interfacial directions.

The driving force has controlled the transportation of crystallizing components during growth process. It becomes effective in two different ways; (1) crystal growth accompanied by phase separation. It is associated with transformation of physical states of the reaction system including liquids (solution-phase) to solids (crystal-phases). Difference in the free energies of physical states may develop a thermal gradient. (2) The high solvent evaporation rate may also facilitate the emergence of higher driving forces. The high driving forces could persuade the branching frequency, yielding more space filling characters in the crystal patterns. Imposed pressures and splay among neighboring crystal fibrils were caused to retain the radial orientations of spherulitic crystals. These were further enhanced by viscous forces and changes in the density during growth process. The Keith-Padden theory has also stressed that the highly enriched liquids were trapped under growing interfaces and some narrow liquid channels separated the adjoining fibrillar crystals towards the spherulite cores. Since the crystals or interfaces were denser than liquids, thus a pressure had developed. Development of pressure function has been found similar to Poiseuille's equation,[4,5] which can keep fibrillar crystals away to coalesced.

The morphology of the spherulites has been examined by SEM as shown in Figure 7. The multiple nucleation centers have been found which self-regulate the forms of spherulites. Two types of crystal organizations have been observed in the spherulitic crystal patterns. Section (a) of the Figure 7 exhibited long crystal fibrils which were diverging from a common center. They formed the main architecture of the spherulitic patterns. These crystals were associated with each other by low-angles and their branching patterns were, found to from the edges. It successively branches to form nearly spherical crystal patterns. Self-assembly mechanism could be supportive to retain isotropy at large scale. The super-saturation condition has been also supported for morphology of spherulitic crystal patterns. On the other hand, numbers of fine crystal fibrils in bundle forms were found which organized to form densely spherical textures, as shown in section (b) of the Figure 7. Some un-organized aggregates have also been observed near the bundles of crystals. This may be residue of metal catalysts or uncrystallized amorphous matters. It might be helpful in binding of the multi- crystal phases together and also serve as a role to molding the spherulitic frames during self-assembly.

Concentration Profiles and Growth Forms of Spherulites. The present experiments have been carried out in wide range of concentrations of organic substrates. The concentrations of acetyl acetone [AA] = 0.230 to 0.276 mol dm^{-3}, and succinic acid [SA] = 0.084 to 0.132 mol dm^{-3} were found effective for growth of branched crystal patters. Results and recorded observations of all experimental conditions were briefly summarized as follows; (1) majority of crystal patterns show branched morphologies, (2) some morphology were found distorted or diffused crystal forms, (3) branching mechanism was found similar to the dendritic crystal patterns, (4) dual substrates were essentially needed

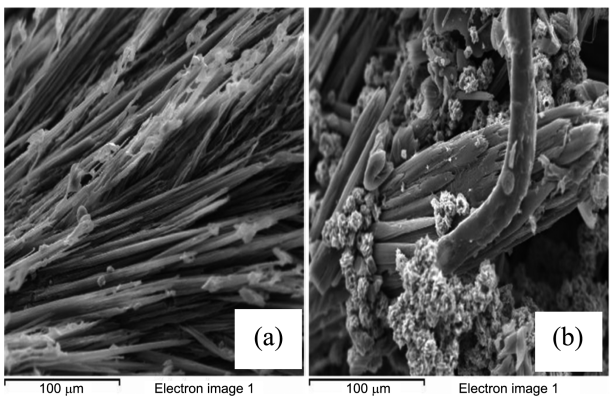

Figure 7. SEM microphotographs, (a) Fibrillar texture, and (b) Crystals in bundle form.

for every sort of experiments for growth of highly ordered and branched crystal patterns.

Additional studies have also been performed in order to examine the morphological transitions in the branched crystal patterns. When, SA was replaced by SAA, seaweed-like crystal patterns analogue to spherulites have also been observed. On the other hand, the rhythmic crystal phases were obtained in the high concentration range of BrO_3^-. The detailed studies and their findings have been summarized in succeeding subsections.

Effect of Substituted Organic Substrate: In this study, SA has been replaced by SAA by keeping all other conditions same as earlier reactions. The concentration ranges, from 0.075 mol dm^{-3} to 0.110 mol dm^{-3} of SAA, were tested. One of best result was obtained at 0.096 mol dm^{-3}. It showed growth of compact and stable structures which exhibited almost spherulitic morphology. Although, they required comparatively much lesser time (approx. 8 hours) for completing the growth process, as compared to earlier reactions. Morphology of resultant patterns has been shown in the Figure 8. It showed broad growing tips that split intermittently; the newly crystals have been found to grow predominately over the others. Splitting of dominant branches was performed in continuous fashions, until the formation of compact and symmetric crystal patterns. The morphology of resulted patterns has been found to be like a seaweed crystallizing patterns.[2] because of their circular shapes they were correlated with the spherulitic crystal patterns.

Optical microphotographs of seaweed-spherulites showed symmetric and compact crystal organizations. The side branches were found broaden which expands up to growing tips. These growing tips have become coarser by additions of newly formed crystal fibrils, as reaction time progressed. The late stage nucleation impinges to others, which results deformation in geometry especially at exterior segments. A graphical scheme has been presented for sea-weed like spherulites, as depicted in the Figure 9. The morphological transition of spherulites is explained as; The SAA has played a key role in the formation of spherulitic patterns. In the earlier reaction, a scope has been assumed by which SA may decompose into SAA. Expense of time must be required for

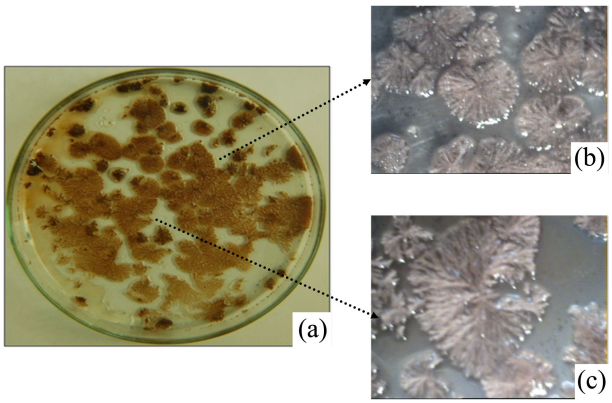

Figure 8. (a) Typical seaweed-like spherulites, and (b) & (c) Optical microphotographs of spherulites.

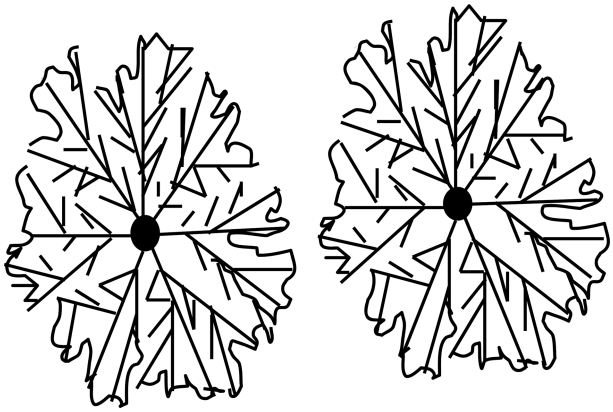

Figure 9. Line drawing graphics of typical sea-weed crystal patterns.

conversions of SAA from SA. In later scheme, the SAA was introduced in the reaction. Thus they grow faster by their direct involvement in the spherulitic structures. It is also evident from growth duration of seaweed-like patterns which required lesser time as compared to dendritic- spherulites. The high solvent evaporation rate has also been observed during the present reactions. This facilitated the emergence of large driving force, which could induce the tip splitting behaviors of sea-weed patterns.

The presence of SAA in the seaweed-spherulitic structure has been supported by GC-MS analysis, as shown in Figure 10. It showed multiple peaks at retention times (min) of 11.64, 12.06, 18.57, and 38.59 with M^+ of 100, 160, 161, and 188 respectively. A prominent peak, at retention time (min.) 11.64 was found to have (100%) ions abundance. The fragmentation patterns of seaweed materials, matched with the data of Wiley registry and NIST mass library database. The fragmentation pattern with M^+ of 100 was found to be similar to SAA (NIST-192). Since SAA showed (100%) ions abundance in the chromatogram so it has been concluded that the SAA certainly takes part in the growth of seaweed-like spherulites.

Effect of Initiator (BrO_3^-) Composition: The BrO_3^- ion is an important reagent for BZ reactions. It initiates the reaction process by forming numbers of intermediates.[29] These intermediates initially controlled the waves and spatio-temporal patterns in solution-phase reaction. Due to excitability

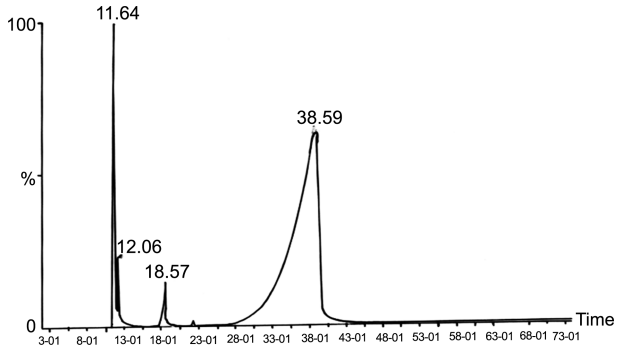

Figure 10. GC-MS chromatogram of sea-weed like spherulitic crystals materials.

and instability characteristics of the reaction, the product phases were diffused from one regime to others. The concentrations of different product phases have been managed by the composition of BrO_3^-. At higher concentration, the production rate of possible product phases might be high. It was observed that the diffusion of products in the reaction media was partially dependent on the BrO_3^-. Because of their usefulness in the BZ reaction, the role of BrO_3^- in the growth of spherulites has been attempted to expatiate.

The concentration range of BrO_3^-, between 0.0448 mol dm^{-3} to 0.0980 mol dm^{-3} has been undertaken for this study. It was observed that at lower BrO_3^-, no spherulites have been formed. At medium concentration range, some irregular branching patterns were observed. Interestingly, at some higher concentration range (nearly 0.0828 M), the rhythmic spherulitic patterns have been obtained, as shown in the Figure 11. The morphology of the rhythmic spherulitic crystal phase has been characterized by optical microscope and it reveals a layered structure. In the core region, the growth of regular spherulites has been found, but as growth process progressed towards periphery, they tend to bifurcates into layers. The spatial gaps between two adjacent layers increased as moving from the core region.

Rhythmic spherulitic crystals were also examined by SEM, which emphases numbers of micro-crystals that assembled linearly to forms fiber-like crystals. The crystal fiber can be formed by adding up a large number of tiny crystal blocks which mechanized through periodic grating. A detailed illustration with SEM microphotograph has been presented in section (a) and (b) of the Figure 12. In the presence of amorphous mass along with rich crystalline matters, the layering structure of spherulites has been grown in such a way that it consists of amorphous mass which is trapped between two crystalline regions. The amorphous mass can produces obstacle to the growth of a regular spherulitic morphology.[30,31] Significance of BrO_3^- may not be ignored for rhythmic spherulites. It starts the reaction initially by formation of intermediates/products. During this; large dynamic fluctuation and high driving forces have been expected. This may distribute the multi product phases at various spatial regions, thus the rhythmic spherulitic patterns have resulted. In detail, the crystal ordering dynamics of

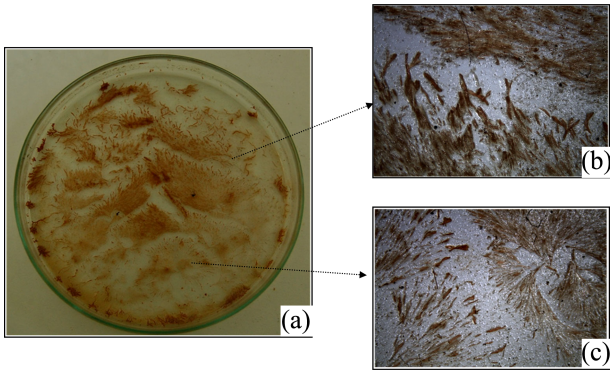

Figure 11. (a) Rhythmic spherulitic crystal patterns, and (b) & (c) Optical microphotographs of rhythmic spherulites.

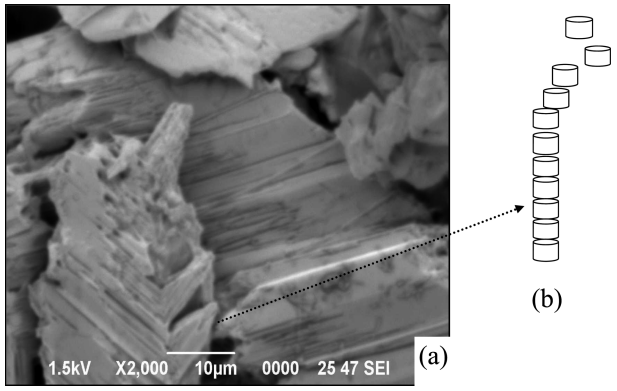

Figure 12. (a) SEM microphotograph of rhythmic spherulites, and (b) An Illustration of periodic grating of crystal blocks.

rhythmic spherulites have suitably been demonstrated in the next section.

Estimated Ordering Dynamics of Rhythmic Spherulites. A stable nucleation included the domains of large thermal fluctuations that attributed very low surface energy.[28,29] These values can also be enhanced quantitatively by Mullins-Sekerka type instability of the reaction media. These factors may trigger the transitions in nucleation geometry of different orderings. It is reported that the nucleation events have occurred in sporadic manner. Each nucleation center grew with their own crystallization rates. Once a stable nucleation center has been formed the growth starts at the interface. This was further monitored by diffusion coefficients of crystallizing units, which have also been dependent on the local free energy of interfaces. Thus, the growth process resulted into a complex ordering profiles of nucleation structures. From this point, the morphology of crystal patterns begins to resolve. The nucleation defects were also effective in the transition of growing crystal patterns. A kind of nucleation defect, which is closely associated with the Kibble mechanism and the interfacial shape dynamics,[32-34] has been preferred for exemplifying their role in the growth of rhythmic spherulitic patterns.

In general, the Kibble mechanism was occurred in those nucleation domains which linked with multi-crystals components of diverse orientations. The high instability and thermal fluctuations were facilitating to trap the crystallizing units in different orderings. Similar topological defects in the nucleation structure have been illustrated in the Figure 13. On the other hand, the interface shape dynamics is driven mainly by anisotropy of the regular structures. The further growth of spherulites from a highly fluctuating nucleation structure has been theoretically predicted by Wulff-Construction Model.[33] It integrates the standard values of growth velocity (V), radius of curvature (R), and driving force (ΔF), are calculated them with the help of crystal growth equation and the radius of curvature dynamic equation. It is useful to predict the crystal orderings in the growth of rhythmic spherulitic patterns;

$$\mu R = \pi r^2 V = -\left(\gamma + \frac{\gamma''(\theta)}{R}\right) + \Delta F \qquad (1)$$

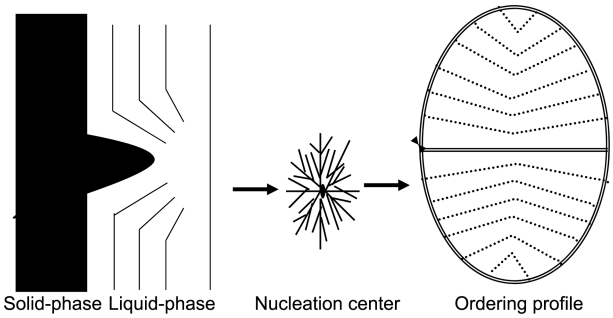

Figure 13. Probable instabilities and crystal ordering profiles during nucleation process.

$$\mu\frac{\partial R}{\partial t} = -\left(\left(\gamma+\frac{\gamma''(\theta)}{R}\right)-\Delta F\right)-R^2\nabla^2\left(\left(\gamma+\frac{\gamma''(\theta)}{R}\right)-\Delta F\right) \quad (2)$$

For simplicity the equations have been written in two dimensional systems. Where μ is the viscosity, θ is the normal angle of interface, and ∇^2 is the Laplace-Beltrami operator.[29,30] At equilibrium, the Eq. (1) is the interfacial balance force equation, also known as the generalized Laplace equation. Eq. (1) denotes the growth driven by a positive free energy (ΔF) that characterizes the phase transformation, which was resisted by capillary forces $\left(-\left(\gamma+\frac{\gamma''(\theta)}{R}\right)/R\right)$ that arise due to curved interfaces. The $-\gamma/R$ term is the Laplace pressure and $-\gamma''(\theta)/R$ is the anisotropic capillary pressure. When (ΔF) dominates, the growth velocity is constant. The Eq. (2) describes the two dimensional curvature dynamics, which follow the transport law for the average curvature H,

$$\frac{dH}{dt} = \frac{1}{2}(\nabla\cdot v) + B\cdot\frac{1}{2}\nabla\cdot((\nabla\cdot v)\cdot k)\pi r^2 \quad (3)$$

Where ν is the interface velocity, $B = -\nabla k$ is the symmetric curvature tensor, k is the interface unit normal, ∇ is the surface gradient profile respectively. Under normal velocity taken as $v = w_\perp$ in two dimensional, the Eq. (3) is simplified as,

$$\frac{dH}{dt} = 2H^2\omega_\perp\frac{1}{2}\nabla^2\omega_\perp \quad (4)$$

Eq. (4) showed that the normal velocity under the two dimensional growth, the radius of a spherulite ($H = -1/R$) followed a linear law;

$$R \propto 2\omega_\perp t \quad (5)$$

From the above equations, it has been suggested that the free energy ΔF dominates over capillary forces, and then the normal velocity $\omega_\perp$ of growing circular crystal interface should be constant. When the radius R follows a linear growth ($R \propto t$), the shape will remain circular ($H = -1/R$). If capillary forces affect the growth, the radius of curvature dynamics R will not be linear longer and a new relation appears $R \propto t^n$, $n \neq 1$.

At the final stage of rhythmic spherulitic patterns, the textures were found to grow continuously with normal velocity, which resulted into perfect curved interfaces. This growth velocity remained constant and can be calculated by Eq. (6) for larger value of R;

$$V = +\Delta F \quad (6)$$

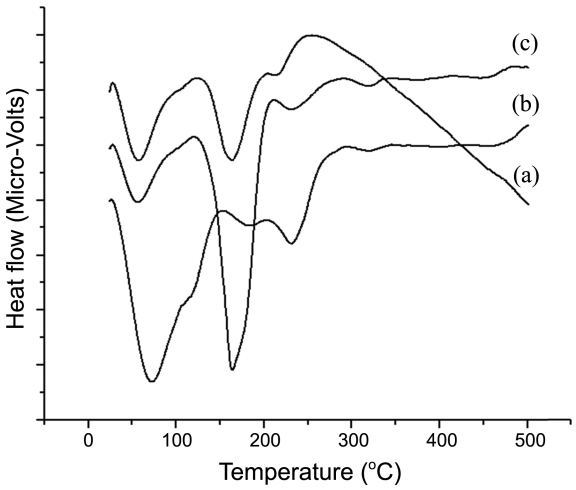

Figure 14. DTA thermogrammes, (a) Dendritic-spherulite, (b) Seaweed-spherulite and, (c) rhythmic sperulite.

It has been concluded that, the rhythmic spherulites may have resulted by the two specific growth rates, faster growth rate followed by a slow growth rate. The growth rates were dependent in the early and late-stage nucleation. During this, the radius has been increased by stepwise fashions. The total free energy densities of growing crystals were also found to decrease rhythmically.[34]

Thermal Analysis. Thermal analyses (DTA) of all three types of spherulitic crystals have been performed in temperature ranges between 0 °C to 500 °C. The DTA thermogrammes were shown in the Figure 14. In the results, multiple and consecutive endothermic peaks have been observed that emphasizes the presence of multi crystal phases in the spherulitic structures. Some exothermic peaks have also been observed, especially in the thermogrammes of seaweeds and dendritic spherulitic materials. This might be due to the reorganizations of crystal forms into different energy evels.[30,35] The DTA curve of seaweed-like spherulites further reveals a stable crystal form compared with others spherulites.

Particle Size Analysis. The average particle size of dendritic-like spherulitic crystals, seaweed-spherulitic crystals and rhythmic spherulitic crystals were carried out by DLS method in multimodal range. The results were shown in the Figure 15, which suggested that the particles sizes have increased when the spherulites are getting in transitions from dendritic morphology to rhythmic spherulites. The larger particle size reveals to a self-organization mechanism which must be undertaken before the spherulitic crystal growths. The particle size in the nano-meter scales were further supported to self-organization in the presence of some short range of intermolecular attraction. Self-selection among the product crystals ultimately facilitate to the formation of fibrous networks in the spherulitic morphologies.[11-13]

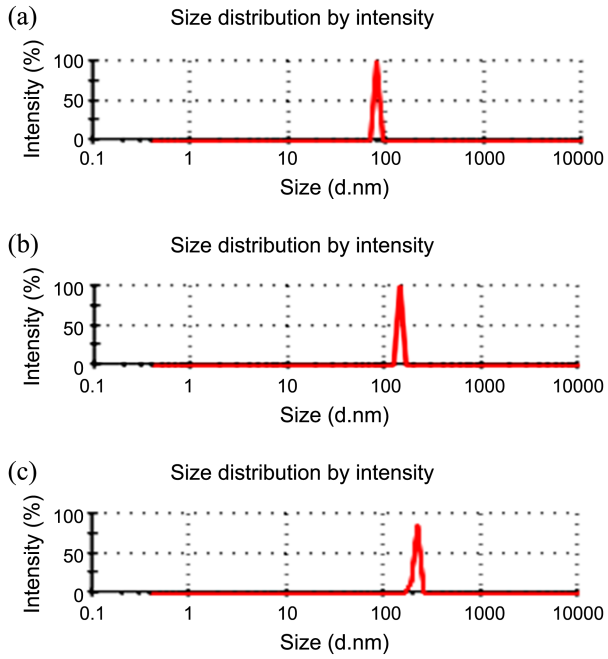

Figure 15. Average particle sizes, (a) Dendritic-spherulite (b) Seaweed-spherulite, and (c) Rhythmic spherulite.

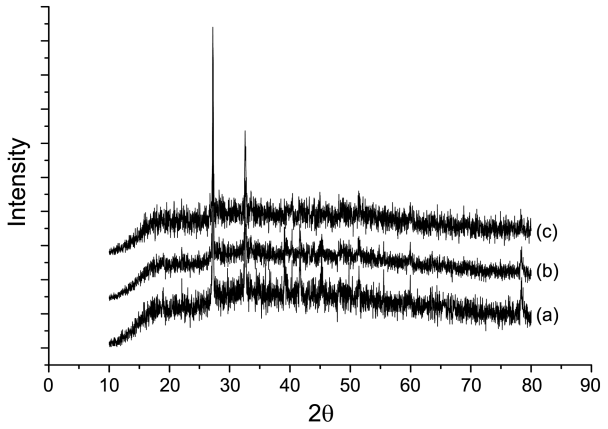

Figure 16. XRD spectra of spherulites in (a) Dendritic-spherulite, (b) Seaweed-spherulite, and (c) Rhythmic spherulite.

X-Ray Analysis. The powdered X-ray diffraction spectra of all three types of spherulitic crystals have been performed and their results were shown in the Figure 16. Evidences of sharp peaks in the region of high intensities were suggested that the spherulitic structures must be composed of majority of crystalline matters. Some broadened peaks were observed in the regions of low intensities that emphasize that the certain amorphous mass have also been trapped in the structures of spherulites.[35,36] The amorphous phase may serve as binding units of multi crystal phases in specific frames during spherulitic crystal growths. The comparison of spectral values of different spherulites which were found to showed that few peaks have appeared in the identical peak positions that attribute to some specific chemical components that played a common role in the formation of all the types of spherulites.

Conclusions

In the present investigation the morphology and growth behavior of spherulitic crystal patterns has been studied in dual substrate of BZ reactions. A colloidal-phase has been observed during reaction process which composed of huge numbers of fine solid particles in the solution matrix. Self-assembly among these colloidal particles have been considered which initially forms fibre-like crystal units, and they further get involved in the growth of spherulitic patterns by self-aggregations. Transitions in morphology of spherulites have also been studied by the effects of substituted organic substrate (SAA) and concentration of BrO_3. Former reactions gave seaweed-like spherulites, while rhythmic crystal phase was obtained in the later reactions. The nucleation mechanism has played a significant role in the transitions of spherulitic morphology, and it has also presented in the studies and properly described.

Acknowledgments. We thank to Dr. Usha Jha, Professor & Head, Department of Applied Chemistry and, Dr. A. K. Chatterjee, Professor & Head, Department of Space Engg. & Rocketry, for their infrastructural supports. We are grateful to Mr. G. K. Prasant, Department of Space Engg. & Rocketry, for his valuable inputs in the improvement of English contents. We also acknowledge Central Instrumental Facility (CIF), Birla Institute of Technology for analytical assistance and their diagnostic reports.

References

1. Granasy, L.; Pusztai, T.; Tegze, G.; Warren, J. A.; Douglas, J. F. *Phys. Rev. E* **2005**, *72*, 011605.
2. Ferreiro, V.; Douglas, J. F.; Warren, J.; Karim, A. *Phys. Rev. E* **2002**, *65*, 51606.
3. Granasy, L.; Pusztai, T.; T. Borzsonyi, T.; Toth, G. I.; Tegze, G.; Warren, J. A.; Douglas, J. F. *Philos. Mag.* **2006**, *86*, 3757.
4. Magill, J. H. J. *Mater. Sci.* **2001**, *36*, 3143.
5. Hutter, L.; Bechhoefer, J. *J. Cryst. Growth* **2000**, *217*, 332.
6. Ryschenkow, G.; Faivre, G. *J. Cryst. Growth* **1988**, *87*, 221.
7. Chow, P. S.; Liu, X. Y.; Zhang, J.; Tan, R. B. *Appl. Phys. Lett.* **2002**, *81*, 1975.
8. Xu, A. W.; Ma, Y.; Colfen, H. J. *Mater. Chem.* **2007**, *17*, 415.
9. Anee, T. K.; Palanichamy, M.; Ashok, M. *Mat. Lett.* **2004**, *58*, 478.
10. Marangoni, A. G.; Ollivon, M. *Chem. Phys. Lett.* **2007**, *442*, 360.
11. Hashimoto, T. *Bull. Chem. Soc. Jpn.* **2005**, *78*, 1.
12. Fukami, K.; Nakanishi, S.; Yamasaki, H.; Tada, T.; Sonoda, K.; Kamikawa, N.; Tsuji, N.; Sakaguchi, H.; Nakato, Y. *J. Phys. Chem. C* **2007**, *111*, 1150.
13. Oaki, Y.; Imai, H. *Cryst. Growth & Des.* **2003**, *3*, 711.
14. Epstein, I. R.; Pojman, J. A.; Steinbock, O. *Chaos* **2006**, *16*, 37101.
15. Epstein, I. R.; Showalter, K. *J. Phys. Chem.* **1996**, *100*, 13132.
16. Toramaru, A.; Harada, T.; Okamura, T. *Physica D* **2003**, *183*, 133.
17. Basavaraja, C.; Kim, N. R.; Park, H. T.; Huh, D. S. *Bull. Korean Chem. Soc.* **2009**, *30*, 907.
18. Salter, L. F.; Sheppard, J. G. *Int. J. Chem. Kinet.* **1982**, *14*, 815.
19. Srivastava, P. K.; Mori, Y.; Hanazaki, I. *J. Phys. Chem.* **1991**, *95*, 1636.
20. Field, R. J.; Boyd, P. M. *J. Phys. Chem.* **1985**, *89*, 3707.
21. Noyes, R. M. *J. Phys. Chem.* **1990**, *94*, 4404.
22. Ruoff, P. *J. Phys. Chem.* **1984**, *88*, 1058.
23. Peralta, C.; Frank, C.; Zaharakis, A.; Cammalleri, C.; Testa, M.;

Chaterpaul, S.; Hilaire, C.; Lang, D.; Ravinovitch, D.; Sobel, S. G.; Hastings, H. M. *J. Phys. Chem. A* **2006**, *110*, 1245.
24. Yadav, N.; Srivastava, P. K. *Cryst. Res. Technol.* **2011**, *46*, 277.
25. Yadav, N.; Srivastava, P. K. *New J. Chem.* **2011**, *35*, 1080.
26. Epstein, I. R.; Pojman, J. A. *Introduction to Nonlinear Chemical Dynamics*; Oxford University Press: New York, 1998.
27. Gomez, A.; Luque, J. J.; Cordoba, A. *Chaos Solitons Fractals* **2005**, *24*, 151.
28. Beck, R.; Andreassen, J. P. *Cryst. Growth Des.* **2010**, *10*, 2934.
29. Kyu, T.; Chiu, H.-W.; Guenthner, A. J.; Okabe, Y.; Saito, H.; Inoue, T. *Phys. Rev. Lett.* **1999**, *83*, 2749.
30. He, Z.; Olley, R. H. *Polymer* **2000**, *41*, 1157.
31. Okada, T.; Saito, H.; Inoue, T. *Polymer* **1994**, *35*, 5699.
32. Gunton, J. D.; Miguel, M. S.; Sahni, P. S. *Phase Transitions and Critical Phenomena*; Academic Press: New York, 1983.
33. Bowick, M. J.; Chander, L.; Schiff, E. A.; Srivastava, A. M. *Science* **1994**, *263*, 943.
34. Wincure, B.; Rey, A. D. *Continuum Mech. Thermodyn.* **2007**, *19*, 37.
35. Zhang, X.; Wang, G.; Liu, X.; Wu, H.; Fang, B. *Cryst. Growth Des.* **2008**, *8*, 1430.